JOURNAL OF AIRCRAFT
Vol. 43, No. 4, July–August 2006

Low-Speed Wind Tunnel Buffet Testing on the F-22

William D. Anderson,* Suresh R. Patel,† and Christopher L. Black‡
Lockheed Martin Aeronautics Company, Marietta, Georgia 30063-0988

DOI: 10.2514/1.10247

Buffet results from the F-22 V-9 model test conducted in the Lockheed–Martin Aeronautics—Marietta Low-Speed Wind Tunnel between May 15 and 18, 2002 are presented. The purpose of the test was to determine the effect on stability and control parameters of computational fluid dynamics derived potential aerodynamic solutions for attenuating vertical tail buffet. Instrumentation was added to permit assessment of the effects of these potential configurations on buffet loads. The data from the test show buffet attenuation benefit from several of the configurations tested, with two fence configurations showing significant reductions in the buffet response up to approximately 32° angle of attack. Computational fluid dynamics analysis predicted significant effects of Mach number, engine inlet mass flow, and scaling on buffet onset. Therefore, any consideration of incorporating such configurations as determined by wind tunnel test should be verified by model testing with these effects present and by full-scale evaluation. Significant buffet attenuation is also shown with side weapons bay doors open. (*Note: The configuration showing most promise for buffet attenuation resulted in a loss in lateral stability at 32°.*)

Nomenclature

b = buffet length scale factor (in)
M = Mach number
Q = dynamic pressure (psf)
S = Strouhal number
V_T = true airspeed
ω = Strouhal frequency (hertz)

Introduction

THE F-22 is a highly maneuverable air superiority fighter with fully integrated fly-by-wire flight controls and thrust vectoring engines. As with other twin tailed fighters [1–5] the F-22 experiences buffeting of its empennage due to vortex flow breakdown forward of the vertical tails.

During the initial phase of the F-22's engineering/manufacturing development, wind tunnel tests were performed on a rigid model to measure the unsteady buffet pressures on the horizontal and vertical tails. These data were used in analysis to predict buffet response and loads on the horizontal and vertical tails for input into static strength requirements, and for the development of a fatigue spectrum.

Early in the flight test program vertical tail response data during windup turns at 18° angle of attack (AOA) and higher showed strong evidence that buffeting of the vertical tails due to vortex impingement was occurring. Early in the flight test program a flight test request (FTR) was written to obtain buffet response data on the structures test aircraft. Data from this testing were used in the structural certification process of the F-22.

During the flight test program it was decided to explore an aerodynamic fix as a possible alternate solution in case the analysis of the buffet flight test data proved the structure to be inadequate. Computational fluid dynamics (CFD) analysis was undertaken to explore the possibility of mitigating the buffeting of the vertical tail using an aerodynamic fix such as a fence similar to the leading edge extension fence used on the F/A-18 [3]. A brief entry into the Lockheed–Martin Low-Speed Wind Tunnel (LSWT) in Marietta, GA was made to evaluate the effect of possible aerodynamic fixes.

The wind tunnel test was conceived primarily to assess stability and control impacts of proposed buffet aerodynamic fixes which had been developed from CFD analysis. The model used was a 1/12 scale aerodynamic performance/stability and control model. To obtain an assessment/preliminary verification of the attenuation effect of these "buffet aerodynamic fixes," four (4) dynamic pressure transducers and four (4) accelerometers were installed on the "rigid" vertical tails. The unsteady pressures measured from the pressure transducers allowed for a quantitative comparison of the buffet forcing function and Strouhal frequency, i.e., key buffet characteristics for each of the configurations tested without the ambiguities of the fin dynamic response that were present in the acceleration response data.

A large number of aerodynamic configurations were selected for testing based on the CFD analysis combined with radar cross section and airframe installation issues. The configurations tested included a fence over the inlet, fences at BL [aircraft butt line (in)] 50, 61, and 74 at several fuselage stations, segmented fences at two locations, strakes on the forebody chine and at the inlet wing intersection, gun door, and two variations at BL 59, and a fin leading edge glove. Open side weapons bay (SWB) doors and inboard 600 gal tanks were also tested to assess their effect on buffet. Also, a qualitative assessment was made on the impact of the preferred concept on horizontal tail buffet by adding an accelerometer to one of the horizontals during the test.

Test data analysis was conducted in near real time, which permitted hands on control of the test, and a thorough workup of the test data and conclusions from the test with documentation within 5 hours of test completion.

Since this test was limited in the available tunnel occupancy hours and instrumentation for measuring buffet response data was limited, a goal of this test was to down select configurations that showed at least a 50% reduction in dynamic response. At the time of the wind tunnel test, flight test buffet data were available only up to 26° AOA. The scope of this test was to cover the full range of AOA available for testing. The highest AOA tested was 42°; however, most testing was limited to 40°.

Computational Fluid Dynamics Analysis

CFD analysis performed at critical flight conditions was initially performed to qualitatively investigate the location of vortex breakdown and its impact on the vertical tail. The goal of using an aerodynamic fix was to delay/eliminate the vortex burst point, or initiate vortex burst earlier (upstream of the vertical tail) to dissipate high energy flow.

Presented as Paper 1678 at the 45th AIAA/ASME/ASCE/AHS/ASC Structures, Structural Dynamics and Materials Conference, Palm Springs, CA, 19–22 April 2004; received 21 April 2004; revision received 25 July 2005; accepted for publication 25 July 2005.

*Principal Engineer. Associate Fellow AIAA.
†Manager, Loads and Criteria.
‡Staff Engineer. Member AIAA.

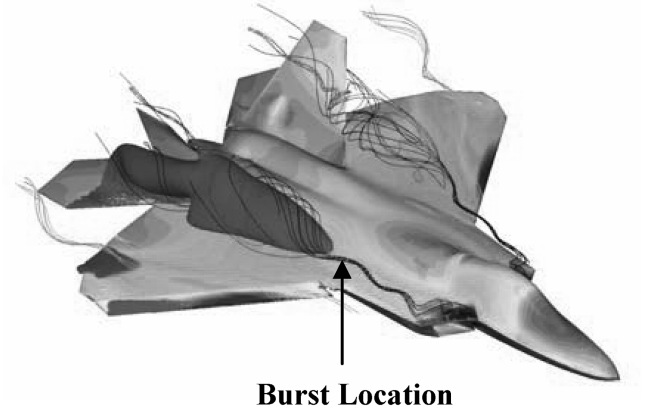

Fig. 1 CFD pressure results for baseline configuration AOA = 22°.

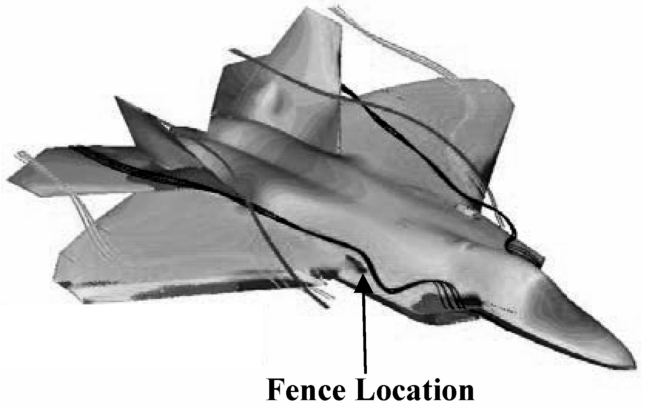

Fig. 2 CFD pressure results for fence configuration 3: fence at the wing root AOA = 22°.

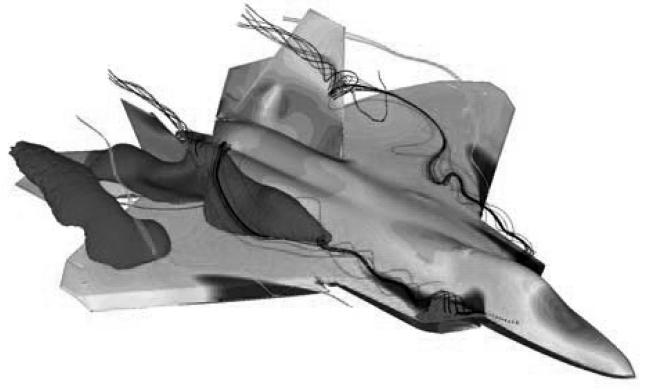

Fig. 3 CFD pressure results for baseline configuration AOA = 26°.

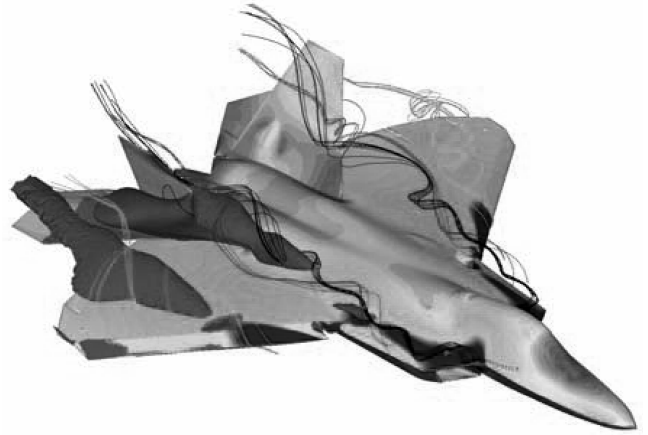

Fig. 4 CFD pressure results for fence configuration 3: fence at the wing root AOA = 26°.

Fig. 5 Installation of fence 10C on model.

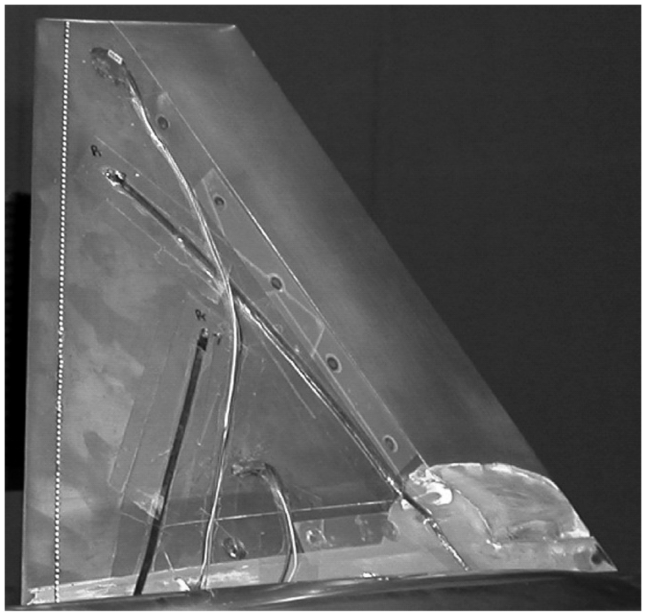

Fig. 6 Instrumentation on inboard surface of right vertical tail.

CFD analyses were initially run at flight conditions of Mach 0.5, Altitude = 13, 700 ft, AOA = 22° and 26°, zero sideslip, and a Reynold's number of 52.9×10^6. The CFD analysis incorporates a full Navier–Stokes solution using the USM3Dns flow solver. Engine inlet mass flow rate were set at military power in the CFD runs.

Figure 1 shows the CFD results from the baseline configuration run at 22° AOA. A strong vortex is seen rising from the junction of the forward fuselage chine and the engine inlet upper lip. Somewhere aft of the junction of the leading edge of the wing with the fuselage, the vortex bursts, embedding the vertical tail in a region of high energy unsteady airflow. A trapezoidal fence was inserted near this point, using geometry identical to that of the F/A-18 fence [3]. In the CFD analysis this fence was located at FS 487, BL 61 and showed an elimination of vortex burst at 22° AOA as shown in Fig. 2.

For 26° AOA the baseline results are shown in Fig. 3, and are similar to the 22° AOA baseline run. However, for the fence configuration at 26° AOA vortex burst is not eliminated as at 22° AOA. As shown in Fig. 4, the vortex burst point has moved further downstream and the burst area has been reduced from the baseline. From a qualitative standpoint this implies lower loads on the vertical

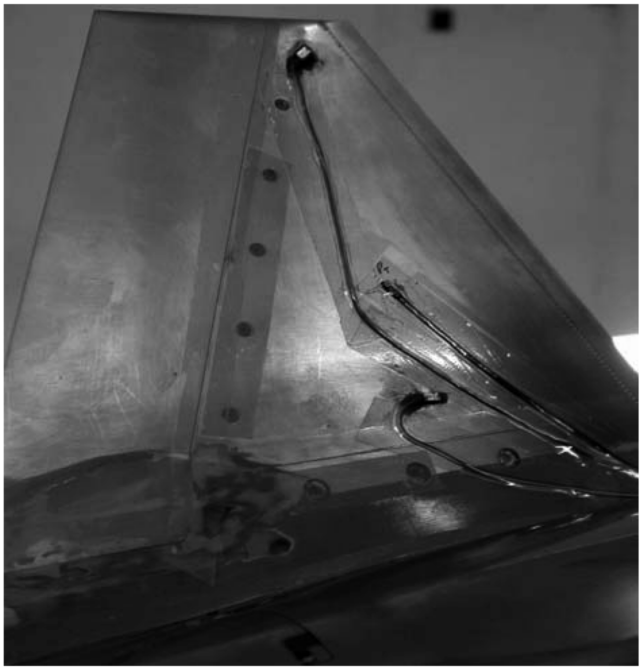

Fig. 7 Instrumentation on inboard surface of left vertical tail.

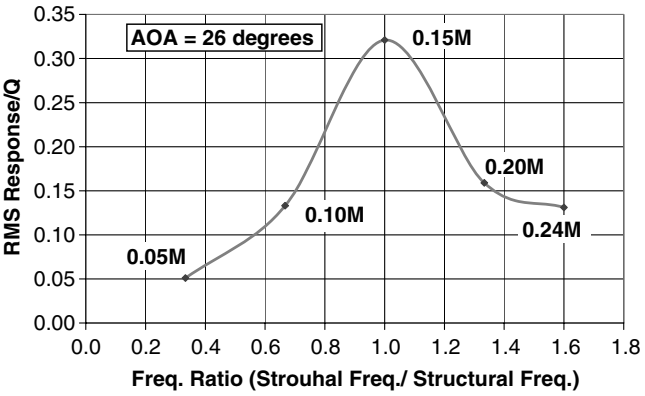

Fig. 8 Model tip response as a function of Mach number and Strouhal frequency.

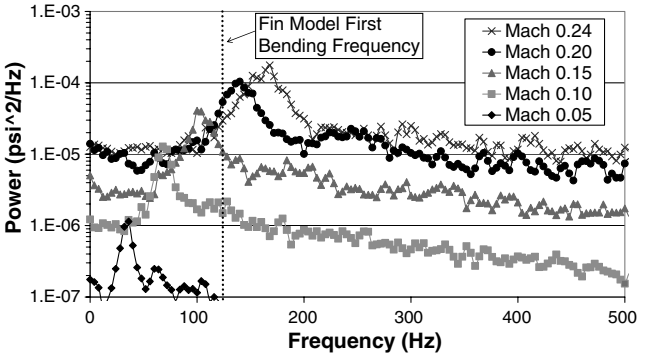

Fig. 9 Variation of PSD with Mach number, AOA = 26°, left inboard midspan pressure tap.

tail. This fence configuration was chosen as the initial location for wind tunnel testing. Several other potential fence configurations were also identified for testing from the CFD analysis.

Note that post test CFD analysis showed that due to the combined effects of Reynolds Number and inlet mass flow rate, the wind tunnel data are skewed 8° to 10° higher in angle of attack than the full-scale data.

Test Description

The V9 aerodynamic performance/stability and control 1/12 scale model was used for this test. The Lockheed–Martin LSWT was used for this test which was conducted between 15 and 18 May, 2002. Most data were obtained for a Mach number of 0.2, a dynamic pressure of approximately 60 psf, and a Reynold's Number of 1.51×10^6. Limited data were also obtained at Mach 0.05, 0.1, 0.15, and 0.24. Data were measured for an AOA range of −10° to 40° and an angle of sideslip range of −8° to +8°. Most data were collected at the nominal leading edge flap setting of 35°.

Approximately 22 configurations were tested of which 5 are discussed here. The configurations include the baseline aircraft model, various fence locations and sizes, strakes, diamond fillets, bay doors open, gun and inlet bleed doors open, a fin leading edge glove, and external tanks. The discussion here is limited to the baseline, to several of the fence configurations, the side weapons bay door open configuration, the fin leading edge glove configuration and inboard external 600 gal fuel tanks.

Various fence configurations were attached to the upper surface of the model to test the aerodynamic impact. Figure 5 shows a typical fence installation: Fence 10C, a trapezoidal fence installed at BL 74 and FS 487, just inboard of the junction of the wing leading edge and the fuselage.

Instrumentation

The rigid vertical tails were equipped with four Kulite pressure transducers and four accelerometers. Since this was an aerodynamic stability and control model, all buffet instrumentation was externally mounted. The right tail was equipped with three pressure transducers —on the tip inboard surface and the tip outboard surface, and the midspan inboard surface. The left tail was equipped with just one pressure transducer at the inboard surface midspan location. Accelerometers were installed on the inboard surface of both tails, at the tip and root. Figure 6 shows the instrumentation on the inboard surface of the right vertical tail while Fig. 7 shows the instrumentation on the inboard surface of the left vertical tail. For all the buffet runs in this test, data were taken on condition for 30 seconds after the model was stabilized.

Data Analysis

Unsteady pressure and acceleration data power spectral densities (PSDs) were calculated real time. The peak PSD responses were determined, as well as the peak PSD frequency for each parameter. These were used to guide the test as the test progressed. A buffet figure of merit was used for a quick quantitative comparative assessment of each configuration. The analysis provided for rapid assessment of configurations and a complete summary of the results from the test in a short period after test completion.

Test Results

Baseline Data

A survey of pressure data was completed for the baseline configuration. A full sweep of AOA from 18° to 40° was done at Mach 0.20. A sweep of Mach from M0.05 to M0.24 was done at 22° and 26° AOA.

Figure 8 shows the fin tip acceleration response as a function of the fin structural frequency divided by the buffet forcing frequency for the 5 Mach numbers in the Mach sweep. This shows the fin is in resonance with the buffeting frequency at Mach 0.15 for the angle of attack of 26°.

Figure 9 presents PSDs showing the impact of Mach number on the left inboard midspan pressure tap. Increasing the Mach number increases the amplitude of the dynamic pressure response and also shifts the peak response frequency. Figure 10 plots the peak response frequency as a function of true air speed (KTAS). The relationship is linear. This linear increase of peak response frequency with true air speed is consistent with Strouhal scaling:

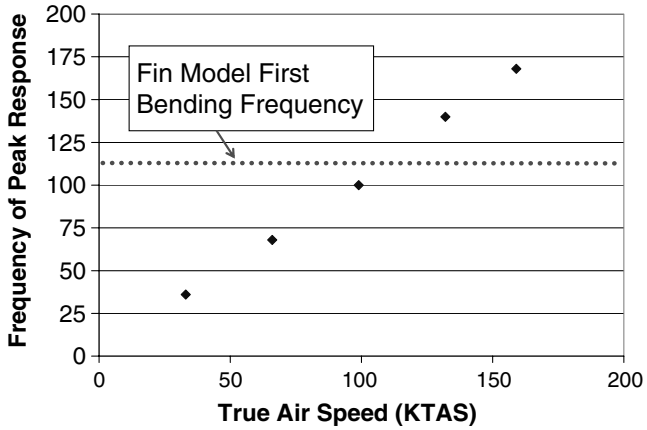

Fig. 10 Strouhal effect of true velocity on response frequency for AOA = 26°, left inboard midspan pressure tap.

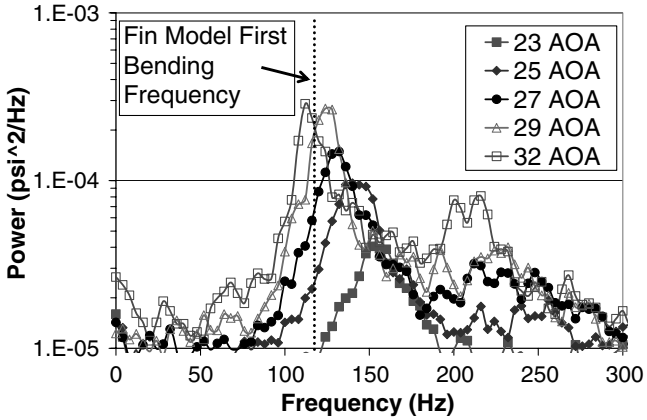

Fig. 11 Variation of PSD with AOA for M = 0.20, left inboard midspan pressure tap.

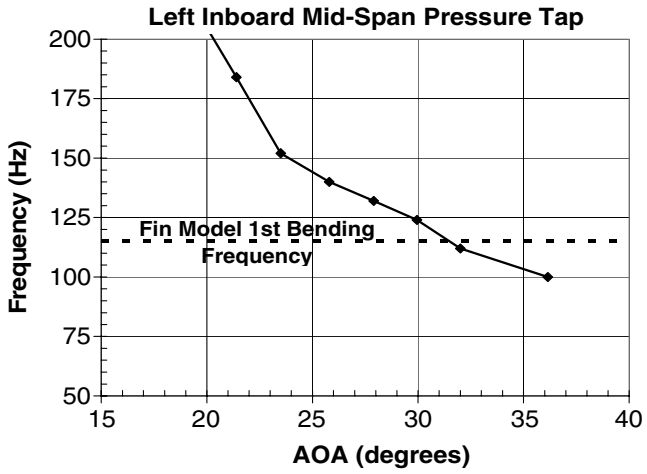

Fig. 12 Strouhal effect of AOA on response frequency for M = 0.20, Left inboard midspan pressure tap.

$$S = \frac{\omega \cdot b}{V_T}$$

These figures also clearly show that the pressure data are not significantly impacted by structural response. At lower true air speeds where the Strouhal frequency is well off the structural resonance, there is no discernible response in the pressure data at the resonance frequency. Therefore, it was not necessary to remove structural contamination from the pressure data.

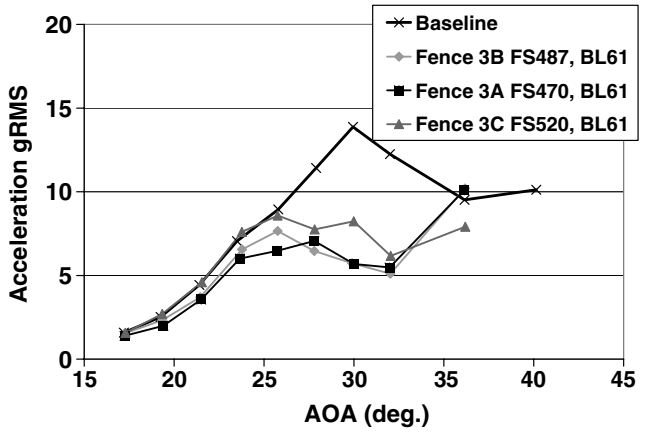

Fig. 13 Effect of fence 3 configurations on buffeting response, left tip accelerometer.

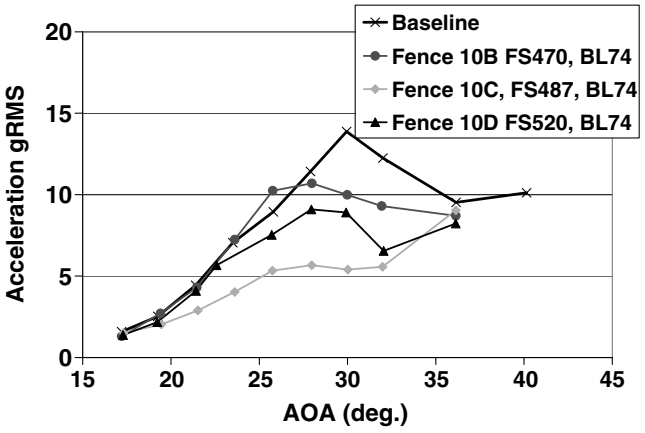

Fig. 14 Effect of fence 10 configurations on buffeting response, left tip accelerometer.

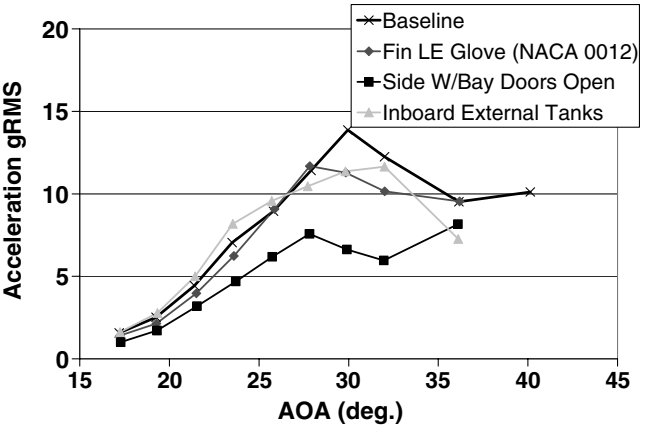

Fig. 15 Effect of other configurations on buffet response, left tip accelerometer.

Figure 11 presents PSDs showing the impact of AOA on the left inboard midspan pressure tap. As AOA increases the peak response frequency decreases. Figure 12 plots the peak response frequency as a function of AOA. This AOA effect is consistent with Strouhal scaling. As AOA increases, the vortex bursts further upstream, increasing the length scale of the vortex. Frequency and length scale are inversely proportional, so an increase in length reduces the frequency.

On each of Figs. 9–12, the fin model structural response frequency is indicated. At M0.20 and approximately 32° AOA, the Strouhal

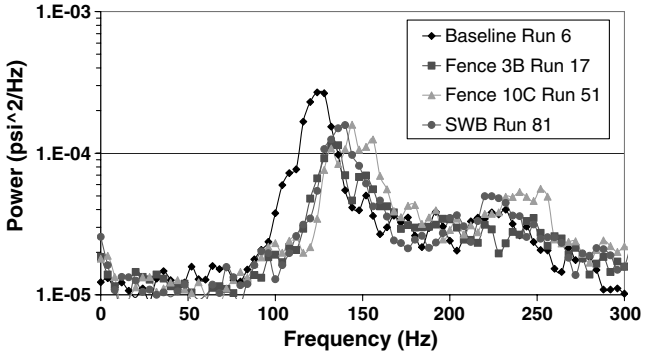

Fig. 16 Effect of configuration on buffet pressure PSD at 30° AOA, left inboard midpressure tap.

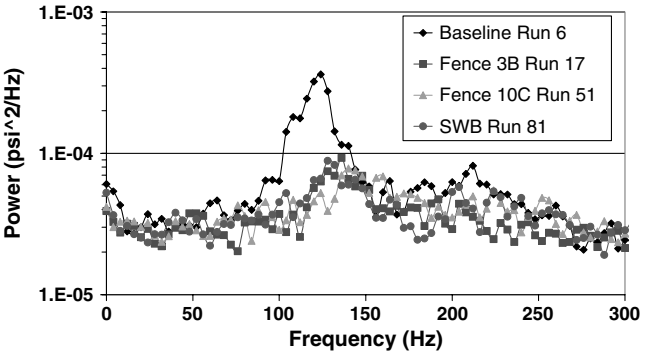

Fig. 17 Effect of configuration on buffet pressure PSD at 30° AOA, right outboard tip pressure tap.

frequency coincides with the structural resonance frequency, producing a maximum possible response. At other speeds and AOAs, the Strouhal frequency moves away from structural resonance, reducing acceleration response. Differing aircraft configurations can also affect the Strouhal frequency by adjusting the length scale of the vortex. Therefore, acceleration response is only a qualitative indication of vortex intensity, and care must be taken in interpreting acceleration results.

Acceleration Data

Top-level results in terms of fin tip acceleration response are summarized in Figs. 13–15. These compare the effect on buffet response of several configurations to the baseline configuration. The response is given in terms of rms of the dynamic acceleration response for each point plotted against the point AOA. The data indicate varied effectivity for buffeting attenuation depending on fence location and type, and other configurations. The acceleration data are qualitative due to the Strouhal Frequency varying with configuration and AOA while the fin structural frequency was fixed. The configurations are grouped as follows: 1) fence 3 at several locations; 2) fence 10 at several locations; 3) other configurations: side weapon bay doors open, leading edge glove, and external tanks.

Fence 3

Figure 13 shows baseline rms accelerometer data versus fence configuration 3. Three fence 3 configurations are compared with the baseline in this plot. All fence 3 configurations were located at aircraft BL 61, but the fuselage stations were varied at FS 470, 487, and 520. From the data shown in Fig. 13, these fence locations provided minor reduction in buffet response up to 26° AOA, and significant reduction from 26° to 32°. From 32° and up, fence 3 response rose back to the baseline response. Fence 3B, located at FS 487, BL 61, was identified as the most promising version.

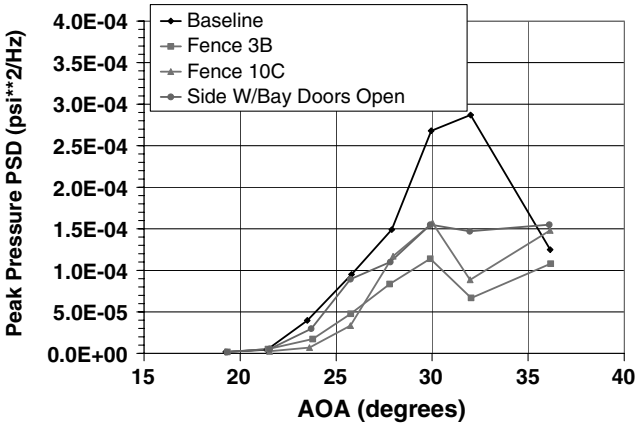

Fig. 18 Variation of peak pressure PSD with AOA at M0.20, left inboard midspan pressure tap.

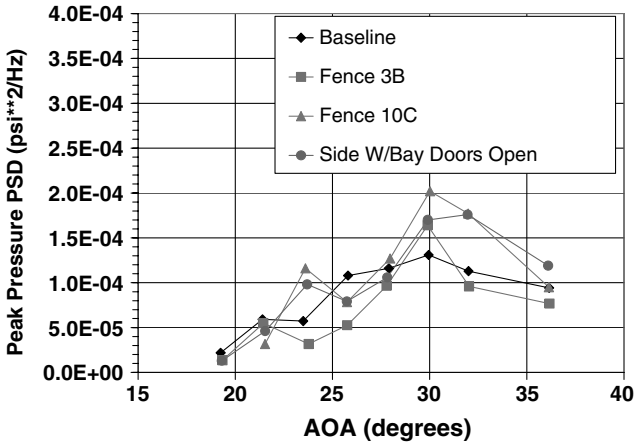

Fig. 19 Variation of peak pressure PSD with AOA at M0.20, right inboard top pressure tap.

Fence 10

Figure 14 shows response data for the baseline versus fence 10 configuration. Again, only 3 variations of fence 10 are shown in this plot. Fence 10 was located at BL 74, outboard of the fence 3 location. The three fore-aft locations were the same as fence 3, i.e., FS 470, 487, and 520. Fence 10C located at FS 487 showed the most reduction in response. Fence 10B showed no decrease in response until 28°, whereas fence 10D showed some decrease above 22° AOA.

Other Configurations

Three other configurations compared with the baseline are shown in Fig. 15. A glove using a NACA 0012 airfoil shape was installed on the fin leading edge to delay leading edge separation. The glove was used as a method of making the leading edge of the fin less sharp to delay airflow separation, to reduce buffet due to separation. As can be seen in Fig. 15, this particular glove was identical to the baseline up to 26° AOA, and showed an approximate 10% reduction in response from 26° to 36°.

The side weapon bay doors were opened as one of the configurations. A reduction in tip response was noted throughout the range of AOA tested. However, it must be noted that the configuration modeled is not truly representative of open weapon bay doors, as this model did not have cavities representing the open bays.

The external 600 gallon fuel tank on the innermost wing station is the ferry configuration, and was tested to note its effect on vertical tail buffet. With external fuel tanks the tip response showed a slight increase up to 26° AOA, and a lower response than the baseline for 26° to 36°.

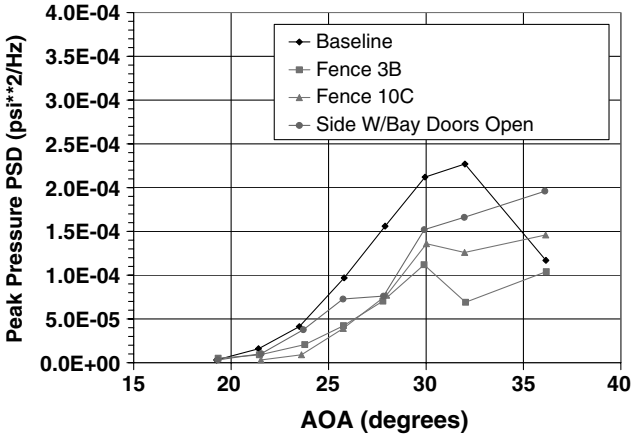

Fig. 20 Variation of peak pressure PSD with AOA at M0.20, right inboard midspan pressure tap.

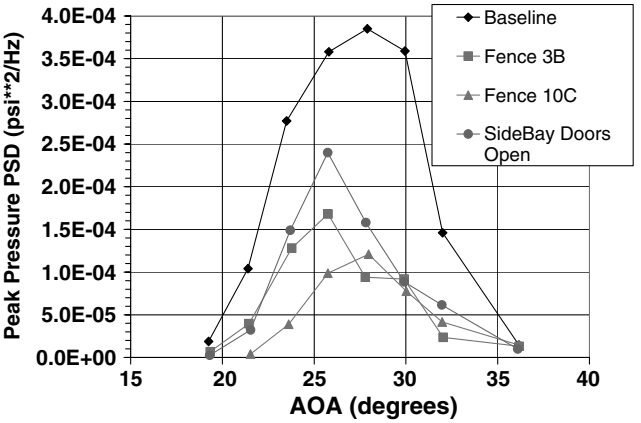

Fig. 21 Variation of peak pressure PSD with AOA.

Pressure Data

Based on the results of the overview, three configurations were chosen for more detailed analysis and examination. The three configurations are the following: 1) fence 3B (run 17); 2) fence 10C (run 51); 3) side weapon bay door open (run 81)

Figures 16 and 17 show pressure PSD plots for these three configurations compared against the baseline for AOA $= 30°$. Figure 16 is PSD data at the left inboard midspan pressure tap and Fig. 17 presents the PSD data at the right outboard tip pressure tap.

It is seen in both of these plots, that a significant reduction in PSD peak amplitude is observed due to both fence configurations, and due to the side weapons bay being open. Note also that not only is the peak PSD decreased, but the frequency of the peak PSD is increased.

Thus, everything else being equal, resonance of the fin with this lower level PSD would occur at a higher true airspeed, and consequently a higher dynamic pressure, providing the aircraft could fly at this higher dynamic pressure at this AOA. This is important, in that any assessment of the effectiveness of any configuration change must take this effect into account.

Figures 18–21 present a comparison of peak PSD value between these configurations and the baseline for each of the pressure taps. The value of the dynamic pressure PSD at the peak response frequency is plotted against AOA for each of the configurations at each of the pressure measurement points.

Figure 18 presents these data at the left inboard midspan location. Note the significant reduction in peak PSD level for the fence and the side weapons bay doors open configurations.

Figure 19 presents the data for the inboard top pressure measurement location. At this location, the baseline levels are low, and the effect of the fences, and side weapons bay doors being open, is to actually increase the peak PSD levels, particularly at the higher angles of attack.

Figure 20 shows similar data for the right inboard midspan location. At this location, the fences and the side weapons bay door open decrease the peak PSD value, with the greater reduction being due to the fences. Fence 3B results in over a factor of 2 reduction in peak PSD response.

It is not clear why the baseline data at this location are lower on the right fin than on the left fin. The measured levels for fence 3B are nearly identical between right and left, the fence 10C results are similar right to left, and right side weapons bay open shows lower peak PSD levels at the lower angles of attack and higher peak PSD levels at the higher angles of attack.

Figure 21 is for the right outboard tip location. The highest baseline peak PSD levels were observed at this location. Also, the greatest effect is seen on reduction in peak PSD levels, particularly due to the fences. Fence 10C shows the greatest reduction by a factor of 3 to 4 in peak PSD level. Fence 3B and side weapons bay open show similar results but give less reduction at the lower angles of attack.

The inboard midspan and outboard tip pressure taps show a larger configuration impact than do the inboard top Kulite.

Each of these configurations is now discussed in more detail, starting with fence 10C.

Fence 10C

Fence 10C generally shows the greatest reduction in buffeting as measured in model fin vibration, rms and peak PSD pressure response, except at the right inboard top Kulite, Fig. 19.

Review of the pressure PSD data, Figs. 18, 20, and 21, for fence 10C indicates the vortex impingement significantly reduced on the fin up to over 30° AOA. Above 32° AOA, the fence loses effectiveness and the buffeting responses approach those of the baseline. A factor of 2 to 4 decrease in buffeting PSD pressure levels with fence 10C is seen. The conclusion is that fence 10C had the possibility of achieving the buffet attenuation goal (2 on rms, 4 on PSD), providing the observed wind tunnel data translated directly to full scale and to higher Mach number and with the correct inlet mass flow.

Fence 3B

Fence 3B also shows a significant reduction in buffeting as measured in model fin vibration and rms and peak PSD pressure response, Figs. 18–21. Again, there is an exception at a limited AOA at the right inboard top Kulite.

Review of the pressure PSD data shows fence 3B reduces the buffet loading on the fin up to over 30° AOA. Above 32° AOA, the fence loses effectiveness and the buffeting responses approach those of the baseline. A factor of 2 to 3 decrease in buffet PSD pressure levels with fence 3B is seen. The conclusion is that fence 3B had the possibility of achieving significant buffet attenuation, but not as much as would be obtained with fence 10C. Again, this is based on the observed wind tunnel data translating directly to full scale and to higher Mach numbers and with the correct inlet mass flow.

Side Weapons Bay Open

The side weapons bay open configuration also showed significant attenuation of buffeting type data. However, this effect was not as significant as with either fence 3B or fence 10C. Some consideration was given to using the side weapons bay doors in this manner but it soon became apparent that this would not be operationally suitable. A key result though is that the data clearly show that at least up to 34° AOA the side bay doors open did not have an adverse effect on fin buffet excitation. It must be noted that the weapon bay cavity was not present in the wind tunnel model.

Results Comparison

The foregoing data show the possibility of obtaining significant buffet attenuation with either the fences or the side weapons bay doors open. These conclusions are valid only if the measured effect is present at Mach numbers up to 0.9 with flight inlet mass flows, at full-scale Reynolds number.

The conclusions are based on very limited data involving 4 dynamic pressure measurement locations, and 2 accelerometer locations. The accelerometer data are qualitative, in that the accelerometer responses are affected by the fixed fin dynamics and the varying aerodynamic Strouhal number as affected by configuration and by angle of attack, creating an ambiguity in accelerometer data. This effect is seen in Fig. 8 which shows the classic resonance response of the fin to the aerodynamic Strouhal forcing frequency. The dynamic pressure data, Figs. 9 and 11, do not contain this ambiguity and therefore provide a better quantitative assessment of the buffeting aeroforces.

A technique was developed that permitted normalizing the data to account for the impact on approximate fin mode excitation/response. This normalizing parameter accounts for the effect of the change in peak frequency on true airspeed/dynamic pressure, the effect of AOA on maximum Q, the PSD level, and an approximation of the integrated effect on modal forcing.

The parameter is separately defined for two flight condition regions. One is where Q is not limited at the peak PSD AOA due to maneuver load factor. This region is typically associated with excitation/response of the lower frequency modes (fin bending and rudder rotation). Here the critical AOA can occur nearly down to sea level. The second flight condition region is where Q is limited by AOA below the critical or peak PSD AOA due to maneuvering load factor limit. This region typically is associated with excitation of the higher frequency modes (2nd and 3rd fin bending and fin torsion).

In the first region, the true airspeed at structural resonance is proportional to the Strouhal number. Therefore the ratio of true airspeeds at structural resonance, comparing one configuration to another, is proportional to the ratio of each configuration's peak PSD frequency. Thus, the ratio of the Qs at resonance at the peak PSD frequency for two different configurations is proportional to the ratio of the peak PSD frequencies squared.

In the second region, load factor is limiting, and the product of Q and AOA is approximately constant. The resonance at the peak PSD is approximately inversely proportional to the AOA at the peak PSD. Therefore, the ratio of the Qs at resonance at the peak PSD frequencies for any two configurations is inversely proportional to the ratio of their peak PSD AOAs.

These considerations and approximations of the generalized forces based on integration of the limited PSD pressure data are used to define a buffet figure of merit for each configuration tested. Data using this parameter is shown in Fig. 22 for several of the configurations tested.

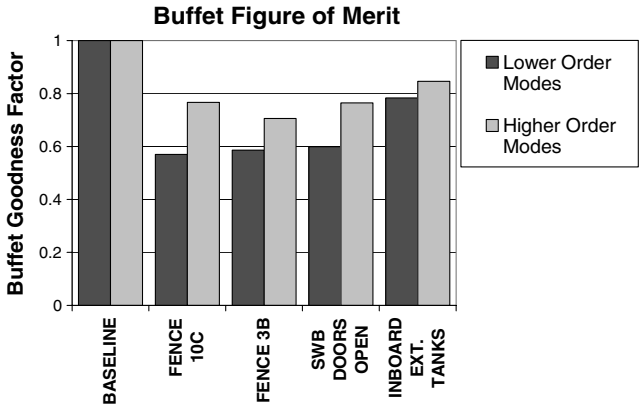

Fig. 22 Buffet figure of merit.

Conclusions

The data from the V-9 low-speed wind tunnel test show both the fence 10C and fence 3B configurations to have strong promise for significant reduction in fin buffet on the F-22 for angles of attack to over 30°. As indicated in Fig. 22, fence 10C is slightly more effective on the lower frequency mode, and fence 3B on the higher frequency mode. Also, the data showed a reduction in buffet excitation due to both side weapon bay doors open and due to the presence of inboard external tanks. These effects would have to be verified by full-scale testing.

Additionally, the limited time in the tunnel did not allow for exhausting every possible means for further optimization of buffet attenuation; nor did the limitations of the low-speed tunnel permit addressing the effects of higher Mach numbers where buffet is critical on the F-22. The assessment of this effect, as well as the effect of flight inlet mass flow must be done if any of these changes were to be incorporated.

It was demonstrated that an assessment of the effect of a large number of configurations on vertical fin buffet can be made with a minimal set of instrumentation and during a relatively short period of test time and analysis. It was also shown, as expected, that some of the test configurations had adverse effects on stability and control. Not surprising was that the configuration with the most benefit for buffet attenuation was shown to have the most negative effect on stability and control.

Acknowledgements

The authors would like to extend their gratitude to the following personnel at Lockheed–Martin Aeronautics, Marietta, GA: Charles Wilson, F-22 Aerodynamics Lead for his assistance with the coordination and implementation of the wind tunnel test, Rick Hooker for running the CFD analysis, Atlee Cunningham of Lockheed–Martin Aeronautics, Fort Worth, for his technical assistance; and Bob Moses of NASA Langley for providing pressure transducers for this test.

References

[1] Zimmerman, N. H., and Ferman, M. A., "Prediction of Tail Buffet Loads for Design Application," Vols. 1, 2, U.S. Naval Air Development Center, Rept. NADC-88043-60, July 1987.

[2] Ferman, M. A., Patel, S. R., Zimmerman, N. H., and Gerstenkorn, G., "A Unified Approach to Buffet Response of Fighter Aircraft Empennage," *Aircraft Dynamics Loads due to Flow Separation*, NATO, Sorrento, Italy, September, 1990; also AGARD Rept. CP-483,

[3] Scanlon, R. W., "F/A-18 Vertical Tail/LEX Fence Dynamic Response Wind Tunnel Test Program," McDonnell Douglas Corporation, Rept. MDC B1393, Jan. 1989.

[4] Triplett, W. E., "Pressure Measurements on Twin Vertical Tails in Buffeting Flows," U.S. Air Force Wright Aeronautical Laboratories, Rept. AFFDL-TR-82-3015, April 1981.

[5] Shah, G. H., Grafton, S. B., Guynn, M. D., Brandon, J. M., Dansberry, B. E., and Patel, S. R., "Effect of Vortex Flow Characteristics on Tail Buffet and High Angle of Attack Aerodynamics of a Twin Tail Fighter Configuration," *High Angle of Attack Technology Conference*, NASA CP-3149, NASA Langley Research Center, Hampton, VA, Oct. 1990.